Interaction of CD44 and hyaluronan is the dominant mechanism for neutrophil sequestration in inflamed liver sinusoids

Braedon McDonald,[1] Erin F. McAvoy,[1] Florence Lam,[1] Varinder Gill,[1] Carol de la Motte,[2] Rashmin C. Savani,[3] and Paul Kubes[1]

[1]Immunology Research Group, Department of Physiology and Biophysics, Institute of Infection, Immunity and Inflammation, University of Calgary, Alberta T2N 4N1, Canada
[2]Department of Pathobiology, Lerner Research Institute, Cleveland Clinic, Cleveland, OH 44195
[3]Department of Pediatrics, University of Texas Southwestern Medical Center, Dallas, TX 75390

The Journal of Experimental Medicine

Adhesion molecules known to be important for neutrophil recruitment in many other organs are not involved in recruitment of neutrophils into the sinusoids of the liver. The prevailing view is that neutrophils become physically trapped in inflamed liver sinusoids. In this study, we used a biopanning approach to identify hyaluronan (HA) as disproportionately expressed in the liver versus other organs under both basal and inflammatory conditions. Spinning disk intravital microscopy revealed that constitutive HA expression was restricted to liver sinusoids. Blocking CD44–HA interactions reduced neutrophil adhesion in the sinusoids of endotoxemic mice, with no effect on rolling or adhesion in postsinusoidal venules. Neutrophil but not endothelial CD44 was required for adhesion in sinusoids, yet neutrophil CD44 avidity for HA did not increase significantly in endotoxemia. Instead, activation of CD44–HA engagement via qualitative modification of HA was demonstrated by a dramatic induction of serum-derived HA-associated protein in sinusoids in response to lipopolysaccharide (LPS). LPS-induced hepatic injury was significantly reduced by blocking CD44–HA interactions. Administration of anti-CD44 antibody 4 hours after LPS rapidly detached adherent neutrophils in sinusoids and improved sinusoidal perfusion in endotoxemic mice, revealing CD44 as a potential therapeutic target in systemic inflammatory responses involving the liver.

CORRESPONDENCE
Paul Kubes:
pkubes@ucalgary.ca

Abbreviations used: ALT, alanine aminotransferase; FL-HA, fluorochrome-tagged hyaluronan; HA, hyaluronan; HABP, HA-binding protein; HNase, hyaluronidase; hpf, high powered field; IαI, inter-α trypsin inhibitor; NETS, neutrophil extracellular traps; RHAMM, receptor for HA-mediated motility; SHAP, serum-derived HA-associated protein; VAP, vascular adhesion protein; VCAM, vascular cell adhesion molecule.

Severe sepsis/septic shock continues to present a dismally poor prognosis in hospital intensive care units, resulting in the deaths of 300,000–500,000 North Americans each year (1). A central contributor to mortality in Gram-negative sepsis is LPS (or endotoxin) (2, 3). Bacterial shedding of LPS into the blood results in inappropriate activation of neutrophils that, regardless of the initial source of infection, become lodged in the capillaries of the lungs and sinusoids of the liver (4). Although antimicrobial treatments have been developed to help combat severe septicemia, in addition to their beneficial effects, antibiotics have also been shown to further increase shedding of LPS into the circulation leading to enhanced inflammation (5, 6). The systemic inflammatory response and multiple organ dysfunction associated with severe sepsis and septic shock continue to elude effective therapies, and mortality rates remain near 50% (7). Thus, understanding the molecular mechanisms of neutrophil sequestration in vital organs such as the liver may help identify novel therapeutic targets to generate new and more effective treatments for septic patients.

Neutrophil recruitment during inflammation is classically attributed to a multi-step cascade involving initial tethering and rolling along the vessel wall, followed by firm adhesion to the vascular endothelium. This paradigm has been extensively studied and is well characterized for vascular beds in tissues such as muscle, mesentery, and skin (8–10). Within the postcapillary vessels of these tissues, the presence of proinflammatory molecules such as LPS induce the classical paradigm of neutrophil recruitment involving selectin-mediated tethering and rolling (E-, P-, and L-selectin), followed by β_2 and during severe sepsis β_1 integrin–mediated

B. McDonald and E.F. McAvoy contributed equally to this work.
The online version of this article contains supplemental material.

firm adhesion (11). The liver presents an apparent exception to this classical paradigm of neutrophil recruitment in three fundamental ways: (a) in addition to the postsinusoidal venules, neutrophils also adhere to the endothelium of capillaries called sinusoids; (b) within the sinusoids, neutrophils appear not to roll for a significant distance, but rather tether and immediately adhere; and (c) the adhesion of neutrophils within the sinusoids was shown to be completely independent of selectins (12, 13). The fact that selectins were not involved in the process of neutrophil recruitment in liver sinusoids led us and others to propose that neutrophils may be sequestered by physical means because of the narrow diameter and low shear forces in these vessels (14–16). Although this is certainly a plausible mechanism, it remains a default position and is almost impossible to prove directly. However, the identification of a molecule that supports adhesion of neutrophils in the sinusoids would minimize physical trapping as a dominant pathway of neutrophil sequestration in these vessels.

There are numerous molecules that may potentially mediate the selectin-independent tethering and adhesion of neutrophils in the liver sinusoids during endotoxemia. First, α_4 integrin supports both rolling and adhesion, but primarily of mononuclear cells under normal conditions (17, 18). However, α_4 integrin has been shown to mediate neutrophil adhesion to vascular cell adhesion molecule (VCAM)-1 under flow conditions in vitro using blood from septic patients, but not from healthy donors (19). β_2 integrin (CD18) is mostly thought to mediate firm adhesion rather than tethering and rolling, yet at lower shear rates (50% reduction) neutrophils can tether, roll, and adhere via CD18 in vivo (20). VAP-1, CD44, CD43, and FcγRIII have all been reported to support leukocyte–endothelial interactions under flow conditions, not to mention other as yet undiscovered adhesive mechanisms (21–24). Finally, it is possible that multiple molecules collaborate, perhaps in an overlapping manner with selectin and integrin functions, to sequester neutrophils in liver sinusoids.

In this study, using a novel biopanning screen for expression levels of known endothelial adhesion molecules, hyaluronan (HA), an important ligand for CD44, was identified as a potential candidate for adhesion because of its selective abundance in the liver sinusoids of both control and endotoxemic mice. Although CD44 has been implicated as a leukocyte adhesion molecule in other organs, its function always overlapped with the classical adhesion molecules (selectins and/or integrins) (25, 26). Herein, we report the unique observation that neutrophil CD44 alone was necessary and sufficient for reversible neutrophil adhesion to HA within liver sinusoids in vivo, and that disruption of CD44–HA interactions reduced liver pathophysiology and damage in response to bacterial endotoxin. The prevailing view to date is that CD44 on endothelium presents HA to activated leukocyte CD44 to induce rolling and/or adhesion. Our evidence suggests that LPS does not induce any significant increase in the avidity of neutrophil CD44 for HA. Alternatively, it has recently been shown that structural modification of endothelial HA via binding of serum-derived HA-associated protein (SHAP) potentiates adhesion to leukocyte CD44 (27). Indeed, increased SHAP expression on HA-bearing sinusoids was detected in endotoxemic mice, indicating that modification of HA had occurred. CD44-dependent adhesion was reversible and not replaced by other adhesive mechanisms or physical trapping, suggesting a key role for molecular adhesion in liver sinusoids.

RESULTS

HA is highly expressed within liver sinusoids

Neutrophil recruitment into the liver sinusoids occurs within 30–60 min after LPS administration (unpublished data), suggesting the possibility that a constitutively expressed adhesion molecule may mediate neutrophil adhesion in these vessels. A biopanning approach using a modified dual-radiolabeled antibody technique was used to examine the expression of numerous adhesion molecules in all major organs. In brief, ^{125}I-labeled antibodies against the adhesion molecule of interest, or HA-binding protein (HABP), were coinjected with ^{131}I-labeled nonbinding isotype control antibodies into either untreated or LPS-treated animals, and the organ-specific expression of the adhesion molecule of interest was determined by measuring ^{125}I levels and subtracting nonspecific binding (^{131}I levels). In addition to corrections for the weight of tissues, selected values were also normalized for organ-specific vascular surface areas from published data in the literature (28). We found that neither VCAM-1, E-selectin, nor P-selectin was expressed under basal conditions in liver vasculature (Fig. 1, B–D). In contrast, HA was expressed in extremely high concentrations in liver but not other organs under basal conditions (Fig. 1 A). The addition of LPS increased VCAM-1, E-selectin, and in particular P-selectin expression in the liver, consistent with the importance of these molecules in postsinusoidal venules during inflammation (Fig. 1, B–D) (13). Vascular HA expression levels remained unchanged in most organs including the liver between untreated and endotoxemic mice (Fig. 1 A). Although the liver has a fenestrated endothelium, a control protein (^{131}I-labeled nonbinding antibody) did not accumulate to the same degree as HABP. Thus, the results cannot reflect nonspecific accumulation of HABP in the liver. Additionally, comparison of vascular HA expression between various organs revealed relatively large amounts of HA in the hepatic vasculature versus other organs. Normalization of HA expression levels from the lung, liver, and heart to values of endothelial surface area demonstrated that vascular HA expression per unit surface area was more than two orders of magnitude higher in the liver versus the lung or heart (Fig. 1 E).

Spinning disk confocal microscopy was used to investigate the location of HA expression within the liver microvasculature. Fig. 2 (A and B) displays the liver architecture of sinusoids and postsinusoidal venules (arrows and arrowheads, respectively), and demonstrates that the amount of autofluorescence produced by the liver is low before the addition of any fluorophore. Treatment with Alexa Fluor 488 HABP to

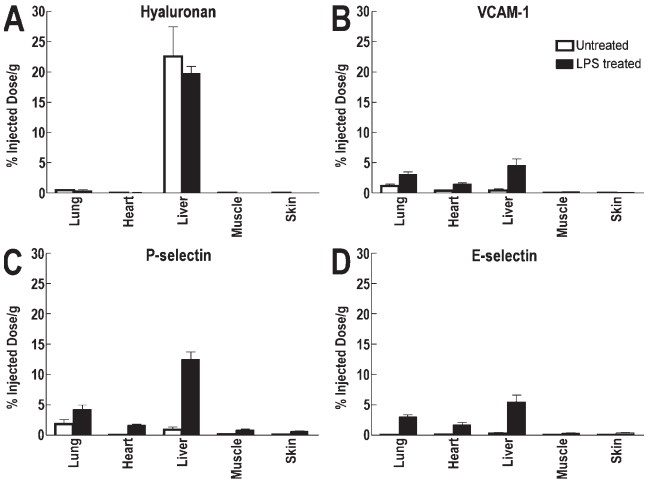

E

	Endothelial Surface Area[1] (cm^2g^{-1})	HA Expression per Unit of Vascular Surface Area [2] ($x10^{-4}$ % injected dose/cm^2)	
		Untreated	LPS
Lung	3000	1.7 ± 0.3	1.3 ± 0.4
Liver	250	904 ± 195	788 ± 48
Heart	500	0	0

[1] From reference 28.
[2] Calculated by dividing values for radioactive HABP binding for each organ (% injected dose/g, from Fig 1A) by the values for endothelial surface area (cm^2g^{-1}) noted in the table.

Figure 1. HA is disproportionately expressed in the liver versus other tissues. A modified dual-radio labeling technique was used to determine the expression of HA (A), VCAM-1 (B), P-selectin (C), and E-selectin (D) on the endothelium of various tissues in both untreated mice and mice treated for 4 h with an i.v. injection of LPS. (E) Values for HA expression in the lungs, livers, and hearts of untreated and LPS-treated animals were normalized to published values of vascular surface area for these organs to compare standardized expression levels between organs. All data are expressed as the arithmetic mean ± SEM.

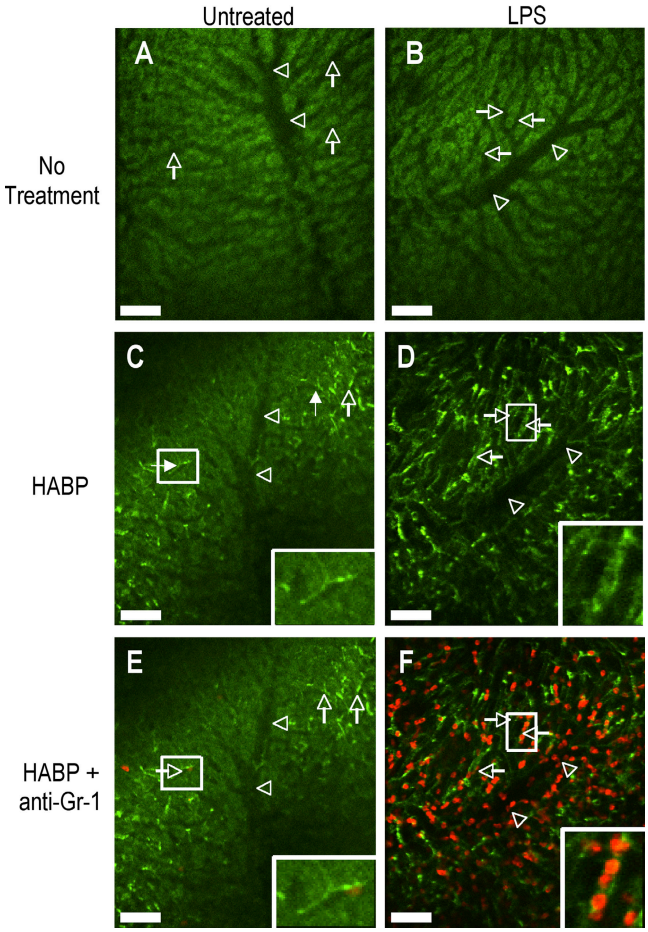

Figure 2. HA is expressed in the sinusoids, but not in the postsinusoidal venules, of the liver. The location of HA expression within the liver microvasculature was determined via fluorescence intravital microscopy of the liver using a spinning disk confocal microscope. Mice were left untreated or treated for 4 h with i.v. LPS. (A and B) The liver architecture shown by autofluorescence before the addition of any fluorophores. HA localization was observed by administration of Alexa Fluor 488–labeled HABP in untreated (C) or LPS-treated (D) mice. PE- labeled anti–Gr-1 antibody was also used to examine neutrophil presence in the liver (E and F). Squares represent areas enlarged in inlay (C–F). Arrows and arrowheads denote the location of the sinusoids and postsinusoidal venules, respectively. Bars, 100 µm. Images are representative of at least three experiments.

detect vascular HA expression revealed significant basal expression of HA in sinusoids (Fig. 2 C, arrows) but not postsinusoidal venules (Fig. 2 C, arrowheads). After LPS administration, HA expression remained restricted to the sinusoids (arrows) and not postsinusoidal venules (Fig. 2 D, arrowheads). The addition of a low concentration of PE-labeled anti–Gr-1 antibody (selectively binds neutrophils without depletion) demonstrated that the presence of HA in sinusoids under basal conditions was not sufficient to induce neutrophil adhesion (Fig. 2 E), whereas LPS administration resulted in neutrophil accumulation in the sinusoids (Fig. 2 F).

HA mediates systemic LPS-induced neutrophil recruitment into sinusoids, but not postsinusoidal venules

Preliminary experiments were conducted to establish that ~25 µg LPS per mouse induced an optimal neutrophil recruitment response in WT animals. This rather low concentration of LPS induced abundant neutrophil adhesion in the liver microvasculature without causing mortality or a dramatic decrease in perfusion. Intravital microscopy was used to show that in the absence of LPS, minimal leukocyte–endothelial interactions occurred in the hepatic vasculature (Fig. 3). Both the number of rolling (Fig. 3 A) and adherent (Fig. 3 B) cells per 100 µm in the postsinusoidal venules increased significantly after 4 h of LPS. Within the sinusoids of LPS-treated mice, adhesion was 14-fold greater than in untreated mice (Fig. 3 C). No rolling was observed in the sinusoids under control or inflamed conditions. To ensure that all rolling and adhering cells were neutrophils, circulating neutrophils were depleted with high concentrations of anti–Gr-1 antibody, and all leukocyte–endothelial interactions were eliminated (Fig. 3, A–D). Furthermore, PE-conjugated anti–Gr-1 antibody (which did not cause neutropenia when used at low

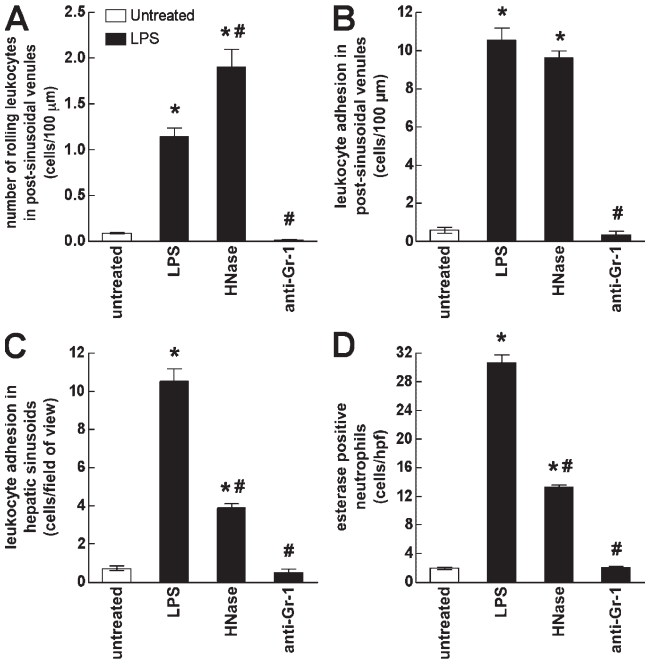

Figure 3. HA mediates neutrophil adhesion in hepatic sinusoids in response to systemic endotoxemia. Untreated WT mice (white bar) and mice treated with LPS i.v. for 4 h (black bar) were compared with WT mice treated i.v. with HNase 2 h before i.v. LPS. One group of WT mice received a neutrophil-depleting concentration of anti–Gr-1 antibody 24 h before LPS treatment. Intravital microscopy was used to measure the (A) number of rolling leukocytes and (B) the number of adherent leukocytes per 100 μm in postsinusoidal venules, and (C) the number of adherent leukocytes per field of view in sinusoidal capillaries. (D) Leder-stained histological sections of livers from untreated and LPS-treated mice were examined by light microscopy, and positively stained neutrophils were counted per hpf (×400) of view. Data are presented as the arithmetic mean ± SEM of at least five animals per group. *, $P < 0.05$ relative to untreated controls; #, $P < 0.05$ relative to LPS-treated WT animals.

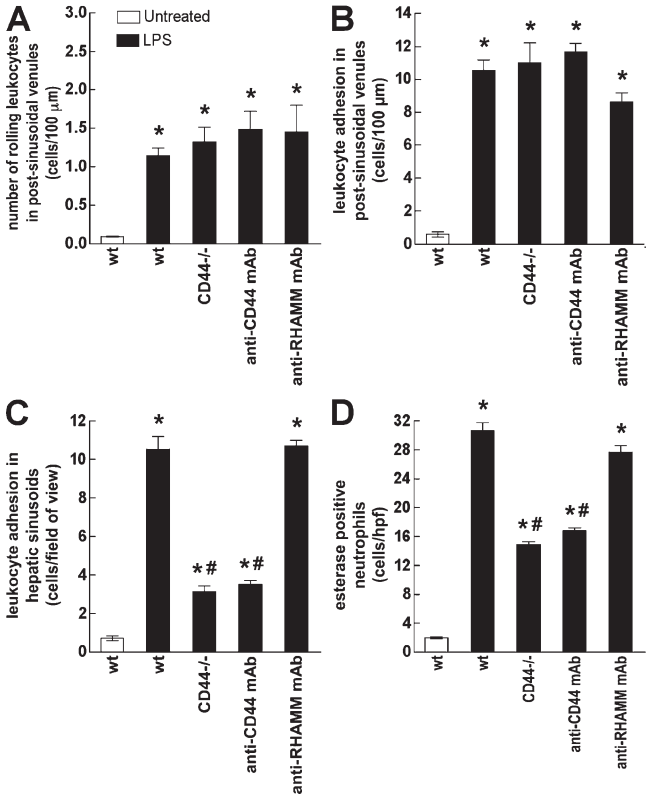

Figure 4. CD44, but not RHAMM, mediates neutrophil adhesion to HA in sinusoids, but not postsinusoidal venules. The numbers of (A) rolling and (B) adherent neutrophils were counted per 100 μm in postsinusoidal venules, and (C) the number of adherent leukocytes in sinusoidal capillaries was determined by intravital microscopy. (D) Leder-stained liver sections were viewed by standard light microscopy, and positively stained neutrophils were counted per hpf (×400) of view. For all parameters, LPS-treated WT (wt, black bar), LPS-treated CD44 knockout (CD44−/−), LPS-treated WT mice injected with anti-CD44 mAb (anti-CD44 mAb), and LPS-treated WT mice receiving anti-RHAMM mAb were compared with untreated WT mice (wt, white bar). Data are presented as arithmetic mean ± SEM of at least five animals per group. *, $P < 0.05$ relative to untreated controls; #, $P < 0.05$ relative to LPS-treated WT animals.

concentrations) confirmed that all leukocytes adhering in the liver after LPS treatment were Gr-1^+ neutrophils (Fig. 2 F).

After each experiment, liver tissue was collected and sections were obtained for histological analysis. Leder-stained liver sections were used to detect those neutrophils that migrated out of the vasculature. Histological examination revealed 30.6 ± 1.1 neutrophils/high powered field (hpf) in the parenchyma of livers obtained from LPS-treated mice compared with 2.0 ± 0.2 neutrophils/hpf in untreated controls (Fig. 3 D). All of the infiltrating cells were neutrophils.

To explore the role of HA in sinusoidal neutrophil adhesion, WT mice were treated with 20 U/g hyaluronidase (HNase) 2 h before LPS administration. This concentration was previously shown to remove HA from the vascular endothelium, as assessed by immunohistochemistry (26). Removal of HA from the endothelium did not decrease neutrophil rolling or adhesion in postsinusoidal venules (Fig. 3, A and B). However, sinusoidal adhesion was significantly reduced in HNase-treated endotoxemic mice compared with endotoxemic mice not receiving HNase (Fig. 3 C). Leder-stained liver sections also revealed a significant decrease in neutrophil infiltrates into the livers of LPS-treated WT mice that received HNase (Fig. 3 D), indicating that HA is an active participant in the sequestration of neutrophils within the inflamed liver.

CD44, not receptor for HA-mediated motility (RHAMM), is the receptor for HA that mediates leukocyte adhesion in the hepatic sinusoids

The adhesive role of HA within the sinusoids presented the possibility that HA-binding receptors including CD44 or RHAMM contribute to neutrophil sequestration in these vessels. There was absolutely no reduction in rolling or adhesion in the postsinusoidal venules of $CD44^{-/-}$ mice or WT mice that received anti-CD44 mAb (Fig. 4, A and B). In stark contrast, a significant 70% decrease in adhesion

within the sinusoids was observed in CD44$^{-/-}$ mice and animals treated with anti-CD44 mAb (Fig. 4 C). Leder-stained liver sections from CD44$^{-/-}$ mice treated with LPS showed a significant decrease in esterase^{+} neutrophils within the liver parenchyma when compared with WT mice treated with LPS (Fig. 4 D). Injection of anti-CD44 mAb 30 min before LPS had the same effect as the CD44 gene knockout (Fig. 4) and the HNase treatment (Fig. 3) for all parameters measured. Because of its role in inflammatory cell recruitment in other tissues, and its redundant function with CD44 in certain contexts (29, 30), we investigated the contribution of RHAMM to neutrophil trafficking in the liver. In LPS-treated mice, the administration of an anti-RHAMM mAb (clone R36) had absolutely no effect on any of the aforementioned neutrophil parameters (Fig. 4). Likewise, vascular adhesion protein (VAP)-1, which mediates Th2 cell adhesion in the sinusoids during Con A–induced hepatitis (24), was found to play no role in neutrophil adhesion in either the sinusoids or postsinusoidal venules in LPS-treated mice (unpublished data). Furthermore, neither anti-RHAMM nor anti–VAP-1 antibody had any additional effect on neutrophil adhesion within the liver vasculature of LPS-treated CD44$^{-/-}$ mice compared with control animals receiving no antibodies (Fig. S1, available at http://www.jem.org/cgi/content/full/jem.20071765/DC1).

Neutrophil, not endothelial, CD44 is important for adhesion in sinusoids

The contribution of endothelial and neutrophil CD44 to sinusoidal neutrophil adhesion after LPS treatment was investigated using BM chimeric mice. BM chimeras were generated by transplanting BM from CD44$^{-/-}$ donors into WT recipients such that CD44 was present on endothelium but not leukocytes, and from WT donors into CD44$^{-/-}$ mice such that leukocytes and not endothelium expressed CD44. Chimeras of WT donor BM into WT recipients were generated as controls. Chimerism had no effect on neutrophil rolling (unpublished data) or adhesion in postsinusoidal venules during endotoxemia (Fig. 5 A). Neutrophil adhesion in the liver sinusoids was unchanged by the absence of endothelial CD44 after LPS administration compared with LPS-treated controls (WT animals that received WT BM) (Fig. 5 B). Conversely, neutrophil adhesion in the sinusoids was significantly reduced in mice with CD44$^{-/-}$ leukocytes compared with controls with WT leukocytes (Fig. 5 B), indicating that neutrophil but not endothelial CD44 is required for adhesion in the sinusoids.

Spinning disk confocal intravital microscopy was used to investigate HA localization in the liver sinusoids in the absence of endothelial CD44. The liver architecture before administration of any fluorophores demonstrated little autofluorescence (Fig. 5 C). Using Alexa Fluor 488–labeled HABP to identify HA in the liver sinusoids of LPS-treated CD44$^{-/-}$ animals, it was found that HA was present in ample quantities lining the endothelial surface despite the absence of endothelial CD44 (Fig. 5 D).

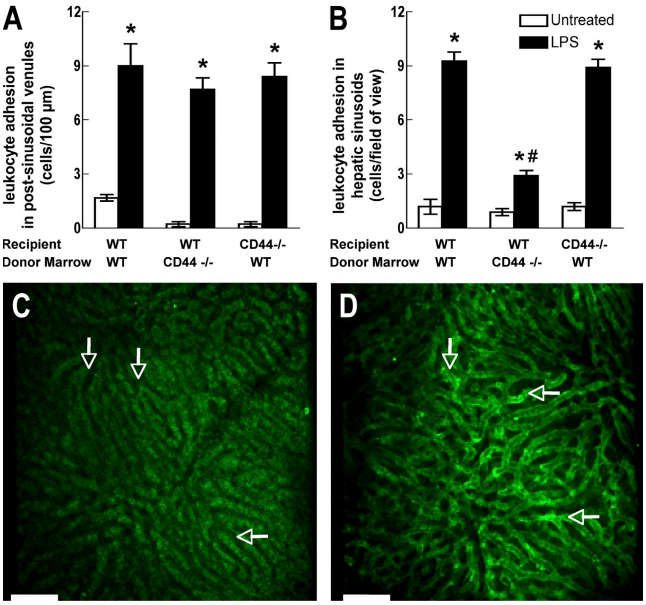

Figure 5. Differential contributions of neutrophil and endothelial CD44 to CD44–HA engagement. (A) The number of adherent leukocytes per 100 µm in postsinusoidal venules and (B) the number of adherent leukocytes in sinusoids per field of view were measured using intravital microscopy in untreated and LPS-treated BM chimeric mice generated in WT or CD44$^{-/-}$ recipients transplanted with either WT or CD44$^{-/-}$ donor BM. Data are presented as standard arithmetic mean ± SEM of at least four animals per group. *, $P < 0.05$ relative to respective untreated group; #, $P < 0.05$ relative to LPS-treated controls (WT recipients with WT marrow). Livers of LPS-treated CD44$^{-/-}$ mice were visualized using spinning disk confocal microscopy to observe (C) the liver architecture shown by autofluorescence before the addition of any fluorophores, and (D) HA localization in sinusoids observed by administration of Alexa 488–labeled HABP. Arrows denote locations of sinusoids. Bars, 100 µm. Images are representative of at least three experiments.

Modification of endothelial HA, but not neutrophil CD44, in response to LPS

To better understand the regulation of neutrophil adhesion in the liver sinusoids, we investigated whether stimulation of neutrophils was sufficient to induce binding of neutrophil CD44 to HA. Using flow cytometry, it was found that treatment of mouse neutrophils with LPS for 4 h was not sufficient to increase mean fluorescence intensity of fluorochrome-tagged HA (FL-HA) binding, whereas direct activation of neutrophil CD44 with a CD44-activating mAb (IRAWB14.4) (31) resulted in high FL-HA binding (Fig. 6 A). Although a small number of neutrophils were observed to have increased binding to FL-HA, neither untreated nor LPS-activated neutrophils rolled on or adhered to immobilized HA under flow conditions in an in vitro flow chamber assay, whereas neutrophils adhered abundantly to immobilized P-selectin (Fig. 6 B). Flow cytometric analysis of neutrophils recovered from LPS-treated mice demonstrated a slight population shift compared with neutrophils from untreated mice (Fig. 6 C), yet this shift did not result in a significant increase in mean fluorescence intensity (Fig. 6 D), nor

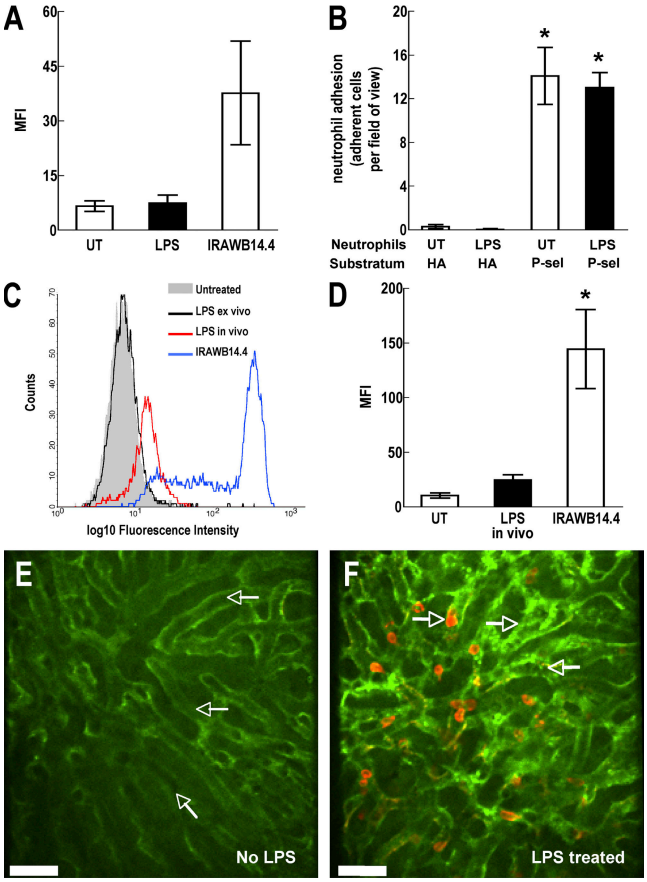

Figure 6. LPS-induction of endothelial HA modification, but not neutrophil CD44 activity. (A) Flow cytometric analysis of FL-HA binding by mouse BM neutrophils left untreated, treated for 4 h with LPS (LPS) ex vivo, or treated with CD44-activating antibody IRAWB14.4 expressed as mean fluorescence intensity (MFI). (B) Adhesion of untreated (UT) and LPS-treated mouse neutrophils on coverslips coated with HA or P-selectin (P-sel; positive control) substratum in an in vitro flow chamber assay. Flow cytometric analysis of FL-HA binding by peripheral blood neutrophils left untreated (UT), treated with LPS ex vivo, incubated with IRAWB14.4, as well as neutrophils from LPS-treated mice (LPS in vivo) expressed as (C) a representative histogram plot and (D) as MFI. All results are representative of at least three experiments. Data are presented as the arithmetic mean ± SEM. *, $P < 0.05$ relative to untreated controls (on HA substratum for B). Livers of untreated (No LPS) and LPS-treated mice were visualized using spinning disk confocal microscopy. (E) The liver architecture shown by autofluorescence before the addition of any fluorophores and (F) SHAP localization observed by the administration of Alexa Fluor 488–labeled anti-SHAP mAbs are visualized. PE-labeled anti-Gr-1 mAb was used to demonstrate neutrophils adherent within sinusoids (E and F). Arrows denote locations of sinusoids. Bars, 50 µm. Images are representative of at least three experiments.

did these cells adhere to immobilized HA under flow conditions (unpublished data). Similarly, neutrophils stimulated with TNF-α, MIP-2, and plasma from LPS-treated mice failed to bind FL-HA, and also failed to roll or adhere to HA in an in vitro flow chamber assay (unpublished data). These data suggest that LPS activation of CD44-HA binding in the liver sinusoids was not likely the result of direct neutrophil CD44 activation by LPS.

Given that neutrophil CD44 activity as well as expression levels of HA in the sinusoids remained constant after LPS administration, we hypothesized that HA may undergo qualitative changes to initiate neutrophil adhesion. Recently, several groups reported that SHAP, composed of the heavy chains of inter-α trypsin inhibitor (IαI), binds to HA via an as yet unknown mechanism, resulting in increased avidity of HA for CD44 (27, 32). Fluorescently labeled antibodies against SHAP (IαI heavy chains 1 and 2) and spinning disk intravital microscopy revealed that SHAP was only weakly detectable in the sinusoids of untreated mice (Fig. 6 E). However, after LPS administration, an abundance of SHAP was observed lining the luminal surface of the sinusoidal endothelium (Fig. 6 F). Furthermore, the addition of an anti–Gr-1 antibody demonstrated the adhesion of neutrophils within the sinusoids of LPS-treated mice at sites where SHAP was present (Fig. 6, E and F).

Attenuation of LPS-induced hepatic injury by diminishing sinusoidal neutrophil recruitment

Fig. 7 shows a quantitative analysis of the pathophysiological dysfunction and hepatocellular injury induced by LPS as assessed by sinusoidal perfusion (Fig. 7 A) and serum alanine aminotransferase (ALT) levels (Fig. 7 B), respectively. Normally, >95% of sinusoids are perfused per field of view in our non-stimulated liver preparation. LPS treatment decreased the number of sinusoids that were perfused to 75–80% (Fig. 7 A). This was determined from recorded videos of intravital microscopy of the liver microvasculature (Video S1, available at http://www.jem.org/cgi/content/full/jem.20071765/DC1). LPS-treated $CD44^{-/-}$ mice, WT mice treated with anti-CD44 mAb, and WT mice receiving HNase all had significantly improved perfusion in sinusoidal capillaries (~90% perfused). Perfusion of sinusoids was also improved in endotoxemic chimeric mice with $CD44^{-/-}$ neutrophils and WT endothelium, but not in chimeras with WT neutrophils and $CD44^{-/-}$ endothelium, consistent with the role of neutrophil but not endothelial CD44 in sinusoidal adhesion (unpublished data).

Methods used in all experiments were designed to avoid rapid mortality and allow the study of patent hepatic vasculature; therefore, only modest levels of LPS were used. Nevertheless, this treatment increased serum ALT levels significantly after 4 h (Fig. 7 B), albeit to a lesser degree than models that cause mortality and severe liver necrosis. However, in LPS-treated $CD44^{-/-}$ mice and WT mice that received anti-CD44 mAb, serum ALT levels were significantly lower than LPS-treated controls (Fig. 7 B). A very similar reduction in ALT levels was obtained from mice treated with HNase (Fig. 7 B).

Two unique and independent neutrophil adhesion mechanisms exist within the liver microvasculature

Fig. 8 A demonstrates that in postsinusoidal venules of LPS-treated mice, the number of rolling neutrophils was reduced by >95% when antibodies to both P- and E-selectin were administered. The lack of rolling cells resulted in fewer

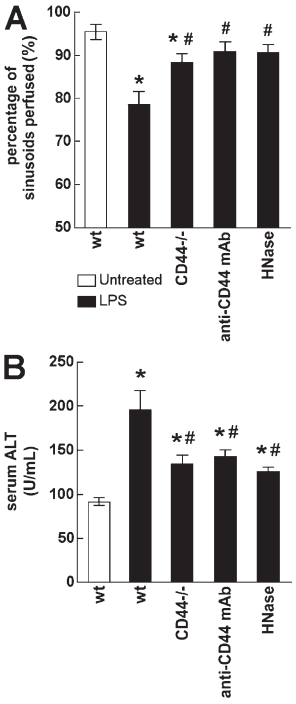

Figure 7. LPS-induced liver injury is diminished by blocking neutrophil adhesion within hepatic sinusoids. The percentage of perfused sinusoids (A) was determined by intravital microscopy, and serum levels of ALT (B) were measured from whole blood as a marker of hepatocellular damage. Untreated WT mice (wt, white bar) and LPS-treated WT mice (wt, black bar) were compared with LPS-treated CD44$^{-/-}$ mice (CD44−/−), WT mice treated with anti-CD44 mAb and LPS, and WT mice treated with HNase and LPS. Data are presented as the arithmetic mean ± SEM of at least five animals per group. *, $P < 0.05$ relative to untreated controls; #, $P < 0.05$ relative to LPS-treated WT animals.

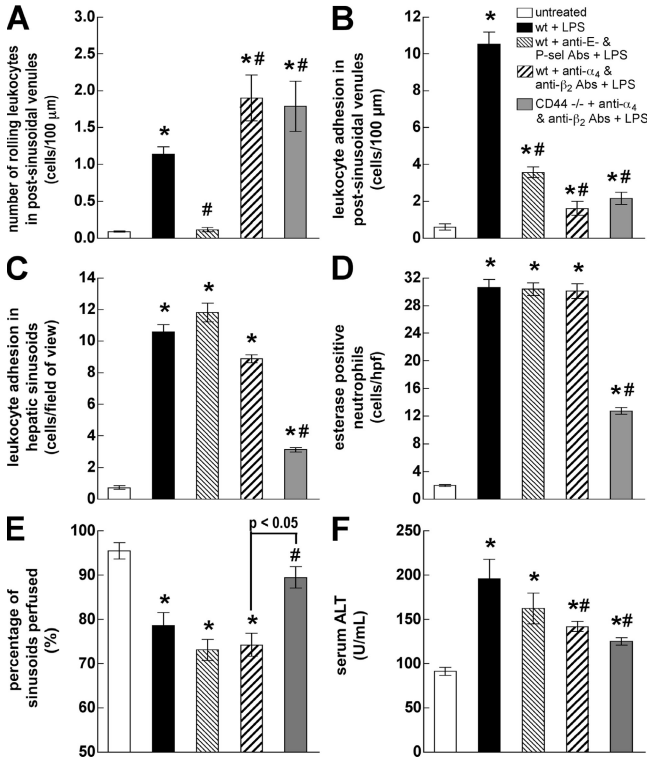

Figure 8. Differential contributions to LPS-induced liver injury by neutrophil adhesion within sinusoids and postsinusoidal venules. The number of rolling (A) and adherent (B) neutrophils per 100 µm in postsinusoidal venules, the number of adherent neutrophils in sinusoidal capillaries (C), and the percentage of perfused sinusoids (E) were determined by intravital microscopy. (D) Leder-stained histological sections of livers were examined by light microscopy, and positively stained neutrophils were counted per hpf (×400) of view. (F) Serum levels of ALT were measured from whole blood. LPS-treated WT mice, LPS-treated WT mice that received E- and P-selectin–blocking antibodies, and WT or CD44$^{-/-}$ mice that received antibodies to block β_2 and α_4 integrins were compared with untreated WT mice. Data are presented as arithmetic mean ± SEM of at least five animals per group. *, $P < 0.05$ relative to untreated controls; #, $P < 0.05$ relative to LPS-treated WT animals.

adherent cells in postsinusoidal vessels (Fig. 8 B). However, as reported previously, selectin inhibition had no effect on neutrophil adhesion in sinusoids (Fig. 8 C). Numerous studies have shown that adhesion of neutrophils to the endothelium of postsinusoidal venules is mediated by integrins, primarily the β_2 integrin CD18 with a varying degree of contribution from α_4 integrin (16, 33, 34). To test for any overlapping functions of CD44 and the integrins, antibodies were administered to both CD44$^{-/-}$ and WT mice to simultaneously inhibit β_2 (CD18) and α_4 (PS-2) integrins. Neutrophil rolling in postsinusoidal venules was not dependent on any of the individual integrins (unpublished data). Tandem inhibition of α_4 and β_2 integrins in WT or CD44$^{-/-}$ mice did not decrease rolling (Fig. 8 A). In WT mice, neutrophil adhesion in the postsinusoidal venules was decreased by ~25% with anti–β_2 integrin antibody, 52% with anti–α_4 integrin antibody (unpublished data), and >80% by dual administration of anti–β_2 and α_4 integrin antibodies (Fig. 8 B). Nearly identical inhibition was seen in CD44$^{-/-}$ mice given anti–β_2 and anti–α_4 integrin antibodies (Fig. 8 B).

Conversely, sinusoidal neutrophil adhesion in WT mice was found to be unaffected by inhibition of β_2 and α_4 integrins (Fig. 8 C). Endotoxemic CD44$^{-/-}$ mice that received both the anti–β_2 and anti–α_4 integrin antibodies had 3.1 ± 0.1 cells/field of view in the sinusoids in response to LPS, a significant reduction compared with WT mice (Fig. 8 C) but not different from CD44$^{-/-}$ mice receiving no antibodies (Fig. 4 C). Surprisingly, histological analysis of Leder-stained liver sections revealed that the number of neutrophils found in the parenchyma of LPS-treated WT mice was the same as LPS-treated WT mice that received the integrin-blocking antibodies (Fig. 8 D). These data demonstrate that the majority of neutrophils that migrate out of the vasculature do so from the sinusoids rather than postsinusoidal venules (because anti-integrin therapies did not impact the number of emigrated cells, whereas lack of CD44 did).

The addition of anti–α_4 and anti–β_2 integrin antibodies had no impact on sinusoidal perfusion (Fig. 8 E). Moreover, anti–E- and P-selectin therapy also failed to affect sinusoidal

perfusion. The addition of the two integrin-blocking antibodies to CD44$^{-/-}$ mice did not further enhance the number of perfused sinusoids (Fig. 8 E) beyond that seen in CD44$^{-/-}$ mice without antibody (Fig. 7 A). Unexpectedly, serum ALT levels were statistically decreased when anti–β_2 and anti–α_4 integrin antibodies were used, despite not affecting neutrophil accumulation in the liver parenchyma (Fig. 8 F). In contrast, using anti–E- and P-selectin antibodies to prevent neutrophil rolling and adhesion in postsinusoidal venules did not improve ALT levels. These findings are in agreement with previous publications showing that β2 and also α4 integrin inhibition can block oxidant production and hepatocyte injury despite failing to block neutrophil recruitment into the liver parenchyma (15, 35, 36). In line with this contention, CD44$^{-/-}$ mice treated with anti–β_2 and anti–α_4 integrin antibody showed the largest decrease in serum ALT levels (Fig. 8 F, last bar), perhaps by blocking integrin function needed for oxidant generation by the few CD44$^{-/-}$ neutrophils that reached the parenchyma. The β_2 integrin appeared to be primarily responsible for this observation (unpublished data).

Leukocyte sequestration in the sinusoids is largely reversible with an anti-CD44 mAb

Although numerous anti-adhesion strategies (e.g., E- and P-selectin blockade) have worked as pretreatments before the establishment of severe inflammation, these same anti-adhesion approaches were less successful as posttreatment therapies (37–39). Nevertheless, the anti-adhesive characteristics of anti-CD44 mAb in the liver sinusoids led us to investigate the feasibility of this approach as a posttreatment. 4 h after systemic LPS administration in WT mice, 20 μg anti-CD44 mAb was injected into the jugular veins of the mice. At 4 h after LPS, ∼10–12 neutrophils could be detected in liver sinusoids (Fig. 9 A). Within 30 min of antibody injection, neutrophils began detaching from the sinusoidal endothelium (Fig. 9 A). This translated into a beneficial physiological outcome as the percentage of sinusoids that were perfused increased significantly after antibody injection (Fig. 9 B).

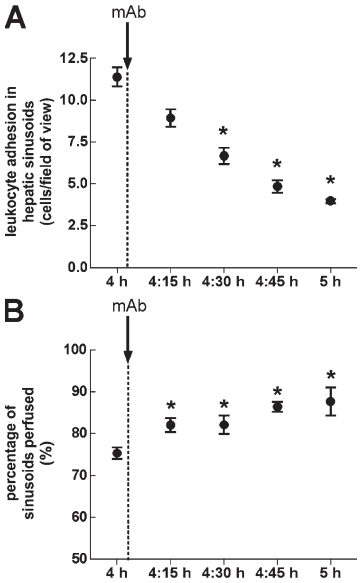

Figure 9. Sinusoidal neutrophil adhesion is reversible by blocking CD44–HA interactions. 4 h after i.v. LPS injection, intravital microscopy was used to visualize the sinusoids of WT mice. After a baseline recording was made, 20 μg anti-CD44 mAb was injected via the right jugular vein, and subsequent recordings were made at 15-min intervals for an additional 45 min. The number of adherent leukocytes per field of view (A) and the percentage of perfused sinusoids (B) were measured. Data are presented as the arithmetic mean ± SEM of at least five animals. *, $P < 0.05$ relative to 4 h LPS (before antibody treatment).

DISCUSSION

Recruitment within the hepatic microvasculature is an exception to the classical recruitment paradigm in that neutrophils are sequestered not only in venules but also in sinusoidal capillaries. Moreover, accumulation of neutrophils in the sinusoids is independent of the selectins known to mediate neutrophil recruitment in tissues such as muscle, mesentery, and skin (8–10, 13, 16). In fact, the prevailing view has been that disseminated release of inflammatory mediators during endotoxemia or sepsis causes increased rigidity of activated neutrophils, causing them to become mechanically lodged in prohibitively small sinusoids (40). In this study, we have demonstrated for the first time that CD44 and its principal ligand HA are intimately involved in the sequestration of neutrophils in the liver sinusoids. Although CD44 has previously been shown to mediate some lymphocyte and neutrophil adhesion, there was always overlapping contributions by other molecules including selectins and integrins, and the mechanism was never dependent exclusively on CD44 (25, 26, 41, 42). In fact, Nandi et al. (25) demonstrated a clear overlap between CD44 and α_4 integrin, which was manifested as a physical colocalization of the two molecules. However, our data in the liver suggested that CD44-mediated adhesion of neutrophils was independent of selectins, α_4 and β_2 integrins, as well as other receptors such as RHAMM and VAP-1, as none of these molecules supported sinusoidal neutrophil adhesion alone or as coadhesion receptors with CD44. Moreover, anti-CD44 antibody was sufficient to block and even reverse adhesion in liver sinusoids, suggesting exclusive adhesion via CD44 in those adherent neutrophils that detached. Much like the liver, extremely high numbers of neutrophils bind within capillary vessels of the lungs during sepsis and endotoxemia. However, in contrast to the liver, HA expression was modest within the lungs, and coincidentally neutrophils still homed to the lungs of CD44$^{-/-}$ animals (unpublished data). This indicates that CD44–HA interactions may be a liver-specific paradigm of neutrophil recruitment during systemic inflammation.

A general biopanning screen for adhesion molecule expression levels drew our attention to the known adhesion molecule HA as a potential contributor to molecular adhesion of neutrophils to sinusoidal endothelium during endotoxemia. Significant numbers of neutrophils adhered in the liver within

30–60 min of i.v. LPS injection (unpublished data), suggesting that the candidate adhesion molecule might be present on the endothelium under basal conditions. This was certainly the case for HA, with levels under basal conditions being at least two orders of magnitude higher than in any other organ even after normalization for weight and vascular density. In addition, spinning disk confocal microscopy revealed selective spatial distribution of HA on endothelial cells of sinusoids but not postsinusoidal venules. This is in agreement with electron microscopy studies in both humans and rats that found HA selectively localized on the apical surface of the sinusoidal endothelium (43, 44). The constitutive attachment of HA to liver sinusoidal endothelium may be distinct from other vascular beds, as the liver functions as a scavenger of HA, continuously binding free HA in the circulation. Indeed, previous studies have reported that microvascular endothelium derived from other organs is not decorated with constitutive HA, and surface expression requires de novo synthesis during the inflammatory response (45).

Previous studies have reported that endothelial CD44 is required to present HA to leukocyte CD44 in a sandwich-like model (26, 41, 46). Unexpectedly, using chimeric mice lacking CD44 on endothelium, we found that endothelial CD44 did not contribute significantly to the binding of HA to liver sinusoidal endothelium. Furthermore, an abundance of HA was observed in the sinusoids of $CD44^{-/-}$ mice. Other endothelial HA-binding receptors have been identified, particularly in the liver. For example, HA receptor for endocytosis (HARE, also designated stabilin-2, FEEL-2), involved in the clearance of HA from the circulation by liver sinusoidal endothelial cells, allows for HA to continuously accumulate on the surface of sinusoids (47, 48). Therefore, HA is constitutively presented to CD44 on neutrophils circulating through the liver. Clearly, in the liver unlike other organs, endothelial CD44 may be dispensable due to the presence of HARE and possibly other unidentified HA receptors.

If HA is constitutively expressed on sinusoidal endothelium and CD44 is constitutively expressed on neutrophils, modification of either HA or CD44 is necessary for active binding in response to LPS. Although CD44 is constitutively expressed on circulating lymphocytes, neutrophils, and other leukocytes, it is normally present in an inactive conformation that does not bind to HA (49). Indeed, many mechanisms for increased affinity and/or avidity of leukocyte CD44 for HA have been identified, including increased CD44 expression, receptor clustering, altered glycosylation, phosphorylation, and sulfation (50). However, many of these findings were derived from studies of lymphocytes and not neutrophils. We found that treatment of neutrophils with LPS, chemokines, TNF-α, plasma from LPS-treated mice, or freshly isolated neutrophils from endotoxemic mice was sufficient for CD18 activation and L-selectin shedding (unpublished data), but not sufficient to induce neutrophil CD44 to adhere to HA. Although a slight shift in the population of neutrophils binding to FL-HA was observed after treatment with LPS, this did not translate into cells adhering to immobilized HA under flow conditions. Thus, LPS-induced activation of neutrophil CD44 is not sufficient for neutrophil recruitment in the sinusoids.

Alternatively, there is new evidence that CD44–HA interactions can be regulated by qualitative changes in HA. For example, alterations of HA polymer length by enzymes or reactive oxygen species liberated during inflammation can modulate the binding of HA to CD44 (51). Additionally, covalent modifications of HA by multiple circulating factors such as SHAP (IαI heavy chains) and extracellular matrix components including versican/PG-M can alter HA matrix organization, leading to increased avidity for leukocyte CD44 (27, 52). Zhuo et al. (27) recently demonstrated that HA–SHAP complexes isolated from arthritic joints increase HA binding avidity for CD44. Interestingly, SHAP was not directly required for cell adhesion, suggesting that it may function to alter HA structure, resulting in increased avidity for CD44. Most relevant to our study was that HA–SHAP complexes were shown to increase lymphocyte binding under flow conditions in vitro at shear stresses <1 dyn/cm^2 (27), which is the physiological shear stress within sinusoids but not postcapillary venules. A striking increase in SHAP deposition on the luminal surface of the hepatic sinusoids only after LPS stimulation but not under basal conditions suggests that endothelial HA is biologically altered through interactions with proteins that may potentiate CD44–HA binding. This supports the hypothesis that LPS may activate CD44–HA engagement in the sinusoids by activating the formation of complexes between endothelial HA and modifying factors such as SHAP in a TLR4-dependent manner, thereby enhancing the avidity of HA for neutrophil CD44. Indeed, our preliminary data suggest that endothelial but not neutrophil TLR4 is necessary for neutrophil adhesion in the sinusoids (unpublished data).

The most clinically relevant finding reported in this study was the observation that sinusoidal neutrophil sequestration and impaired perfusion resulting from 4 h of endotoxemia was rapidly ameliorated by acute administration of an anti-CD44 mAb. Within 1 h of administration, antibody treatment effectively reversed the neutrophil adhesion in sinusoids and significantly improved perfusion through these conduits. Although it was thought that neutrophils that adhere firmly to substratum form a subjacent space that is impenetrable to proteins including proteases and antibodies, we now know that at least in the cremaster and brain vasculature, neutrophil adhesion is dynamic and includes some crawling under flow conditions in vivo (53), which renders the formation of an impenetrable subjacent space less likely.

The reasons for the disproportionate neutrophil sequestration in the liver and lung in response to bacterial endotoxin are not fully understood, but recent evidence suggests that neutrophils home to liver and lung capillaries during endotoxemia and sepsis as an antibacterial mechanism whereby neutrophils enhance the capture of bacteria from the circulation. Neutrophil arrest within the liver sinusoids allows for

the release of webs of DNA called neutrophil extracellular traps (NETS) that ensnare blood-borne bacteria during sepsis (54). However, NETS are covered with bactericidal proteases that may inadvertently cause hepatotoxicity. We therefore hypothesize that neutrophil sequestration within liver sinusoids is a well-coordinated, programmed, innate immune survival mechanism during sepsis that occurs at the expense of damage to the liver. Thus, although blockade of CD44–HA interactions diminished neutrophil-mediated damage to the liver during endotoxemia, this treatment may also affect various aspects of the physiological antibacterial response in the liver. With the advent of antibiotics, tissue injury associated with this mechanism of bacterial trapping via NETS may be therapeutically preventable without increasing susceptibility of the host to infection. Our findings help further the understanding of neutrophil recruitment within the microvasculature of the liver, and suggest potentially useful approaches for the development of therapeutic strategies to combat pathological hepatic inflammation.

MATERIALS AND METHODS

Animals. Experiments were performed using CD44-deficient mice (55) or their respective WT strain (B6129) maintained in a pathogen-free facility at the University of Calgary Animal Resource Center. At the time of use, mice weighed between 20 and 35 g and were 6–10-wk old. All animals were anesthetized with a mixture of 200 mg/kg ketamine (Rogar/STB) and 10 mg/kg xylazine (MTC Pharmaceuticals) administered via an i.p. injection. Experimental animal protocols performed in this study were approved by the University of Calgary Animal Care Committee and met the guidelines of the Canadian Council for Animal Care.

Quantification of adhesion molecule expression. A biopanning screen of adhesion molecule expression levels within the vasculature of major organs of untreated mice, or mice treated for 4 h with an i.v. LPS injection, was performed using a modified dual-radiolabeled antibody technique (56, 57). HA expression was measured using an HABP (Seikagaku) and a nonbinding control protein (nonbinding rat IgG1 antibody control; BD Biosciences). In addition, P-selectin, E-selectin, and VCAM-1 expression were also measured. The HABP and anti-adhesion molecule antibodies were labeled with ^{125}I, whereas the isotype control antibodies were labeled with ^{131}I using the Iodogen method (56, 57).

Animals were injected with a mixture of 10 μg of ^{125}I labeled P-selectin (RB40.34; BD Biosciences) and a variable dose of ^{131}I-labeled nonbinding antibody (BD Biosciences) calculated to attain 400,000–600,000 cpm (to a total volume of 200 μl). The same approach was taken in separate animals to measure E-selectin (9A9; provided by B.A. Wolitzky, Hoffmann-La Roche, Nutley, NJ), VCAM-1 (MK1.9.1; Bayer Laboratories), or HA expression. The labeled HABP and/or antibodies circulated for 5 min, at which point the animals received a heparin bolus (40 U) and were rapidly exsanguinated with a bicarbonate-buffered saline solution. The organs were immediately harvested and weighed, and the ^{125}I and ^{131}I levels in the plasma and tissue of interest were determined. By subtracting the nonspecific control antibody measurements (^{131}I) from the adhesion molecule–specific antibody or HABP measurements (^{125}I), quantitative assessments of expression levels of the various adhesion molecules in tissues were obtained. Adhesion molecule data are expressed as the percentage of the injected dose of antibody per gram of tissue. This technique has been shown to detect endothelial, not extravascular, adhesion molecule expression. Nonspecific binding is accounted for with the nonbinding antibody. Even very low levels of adhesion molecule expression under basal conditions can be detected, as is evident from the fact that mice deficient for the protein being detected (e.g., P-selectin or E-selectin) had values of zero and were significantly lower than basal levels in WT mice (57, 58).

Generation of chimeric mice. BM chimeras were generated according to a standard protocol (41). B6129 and CD44$^{-/-}$ mice were used as recipients and/or donors for sex-mismatched BM transplantation. BM was isolated from male donor mice killed by cervical spine dislocation. Female recipients were irradiated with two doses of 5 Gy (Gammacell 40 ^{137}Cs γ-radiation source), with a 3-h interval between doses. 8×10^6 isolated male BM cells were injected via the tail vein into female-irradiated recipient mice. Transplanted mice remained in germ-free microisolator cages for 8 wk to allow full hematological reconstitution. Previous studies using this method have confirmed that ~99% of circulating cells were from donor marrow, as shown using Thy-1.1 and Thy-1.2 congenic C57B6 mice. Furthermore, in these sex-mismatched transplants, chimerism was confirmed by analyzing leukocytes with fluorescent in situ hybridization for chromosome Y using a star-FISH chromosome painting kit (Cambio). A control transplant between male donor B6129 and female recipient B6129 was used to ensure that no untoward effects of transplantation occurred.

Intravital microscopy in the mouse liver. The procedure for intravital microscopy of the mouse liver was performed as outlined previously (13, 59). After general anesthesia, the right jugular vein was cannulated for administration of additional anesthetic and for injection of antibodies in some experiments. Throughout all procedures the body temperature was maintained at 37°C using heat lamps.

Rolling leukocytes were defined as white blood cells with a slower velocity than the erythrocytes and a detectable rolling motion. Rolling flux was measured as the number of rolling cells per minute, and the velocity of rolling cells was calculated from the time taken to traverse 100 μm. Leukocytes that remained stationary on the venular or sinusoidal endothelium for 30 s or longer were considered adherent cells. Adherent cells were counted per 100 μm in postsinusoidal venules, or per field of view in sinusoids. Percent (%) perfusion of sinusoids was determined by dividing the number of perfused sinusoids by the total number of sinusoids per field of view.

Detection of HA and SHAP by spinning disk confocal microscopy. In some experiments, at the end of a control period or 4 h after LPS treatment, a fluorescently labeled (Alexa Fluor 488 Protein Labeling kit; Invitrogen) HABP (EMD) was injected i.v. to detect localization of HA in the liver microvasculature. In separate experiments, control and LPS-treated mice received fluorescently labeled (Alexa Fluor 488 Protein Labeling kit; Invitrogen) antibodies against SHAP (anti-IαI heavy chains 1 and 2 mAbs; Santa Cruz Biochemicals), the SHAP, known to increase adhesiveness of HA. Localization of SHAP in the liver was used as a detector of HA modification. Mice also received a neutrophil-specific PE-labeled anti–Gr-1 antibody (clone RB6-8C5; BD Biosciences). Intravital microscopy was preformed as described above, and the posterior surface of the liver was viewed with a spinning disk confocal microscope. Images were acquired with an upright microscope (BX51; Olympus) using a 10 or 20×/0.75 N.A. air objective. The microscope was equipped with a confocal light path (WaveFx; Quorum) based on a modified Yokogawa CSU-10 head (Yokogawa Electric Corporation). The liver and infiltrating neutrophils were imaged using either 488 or 561 nm laser excitation (Cobalt), respectively, and visualized with the appropriate long pass filters (Semrock). Typical exposure times for 488 and 561 nm laser excitation were 990 and 617 ms, respectively. A 512 × 512 pixels back-thinned EMCCD camera (C9100-13; Hamamatsu) was used for fluorescence detection. Volocity Acquisition software (Improvision) was used to drive the confocal microscope.

Experimental protocol. For each experiment, mice received between 20 and 35 μg (1 mg/kg) purified LPS from *Escherichia coli* 111B4 (EMD) in sterile saline administered i.v. 4 h before intravital microscopy. This concentration was sufficiently low so that all animals survived general anesthesia, and perfusion in the liver vasculature remained such that leukocyte–endothelial

interactions occurred under flow conditions. In some experiments, mice were injected with either 20 μg of purified anti–mouse CD44 (clone KM81) mAb (Cedarlane), 20 μg of purified anti–mouse β_2 integrin (CD18) antibody (GAME 46; BD Biosciences), 25 μg anti–α_4 integrin (CD49) antibody (PS-2; provided by Merck), a cocktail of 30 μg anti–E-selectin (9A9) and 20 μg anti–P-selectin (RB40.34; BD Biosciences) antibodies, or 100 μg anti-RHAMM antibody (R36), each administered i.v. 30 min before LPS injection. One group received 150 μl of an anti–Gr-1 antibody (clone RB6-8C5; eBioscience) i.p. 24 h before LPS, a treatment previously shown to deplete 95% of neutrophils in mice (59). These concentrations of antibodies were all derived from previous dose response experiments in our laboratories that are published elsewhere (29, 33, 41, 60). In one set of experiments, 20 μg anti-CD44 mAb was administered via the jugular catheter 4 h after LPS. A final group of animals was injected i.p. with 20 U/g HNase type-IV (Sigma-Aldrich), a procedure we previously determined to deplete HA from the vascular endothelium (61). The liver was then prepared for intravital microscopy, and leukocyte kinetics were investigated as described above.

Biochemical assessment of liver injury. Serum levels of ALT were detected in blood obtained via cardiac puncture as an indicator of hepatocellular injury. A commercially available diagnostic kit (Cedarlane) was used to quantify serum levels of ALT. Results are expressed as international units per milliliter of serum.

Histology. The left liver lobe was removed after intravital microscopy and placed in 10% neutral-buffered formalin (Sigma-Aldrich). The formalin-fixed tissue was then embedded in paraffin, cut in 4-μm sections, stained with a chloroacetate esterase (Leder) stain (Sigma-Aldrich), and viewed at a magnification of 400 with light microscopy. Positively stained neutrophils in the liver parenchyma were counted per hpf. The results are expressed as the mean number of cells over 20 fields of view.

Mouse neutrophil isolation for flow chamber and flow cytometry experiments. Mouse BM-derived neutrophils were isolated as described previously (41). After the mice were killed, the femurs and tibias were removed. The ends of the bones were resected, and 10 ml of cold PBS was perfused through the bone to collect the marrow. A discontinuous Percoll gradient was then used to isolate purified mouse neutrophils. Cells were resuspended in HBSS containing 10% mouse plasma at 1.0×10^7 cells/ml. Using this technique, neutrophil populations are ≥95% pure and ≥98% viable (unpublished data).

In vitro flow chamber assay. The parallel-plate flow chamber assay for leukocyte recruitment to HA and P-selectin was used as described previously (26). In brief, rooster-comb HA (Sigma-Aldrich) or P-selectin (R&D Systems) was immobilized on a 35-mm cell culture dish (Corning). The plates were then blocked for 1 h at 37°C with 1% bovine serum albumin (Sigma-Aldrich). BM-isolated neutrophils (10^7 cells/ml) were either left untreated or incubated at 37°C for 4 h with 100 ng/ml LPS. Cells were then perfused across the substratum at a constant shear rate of 0.2 dynes/cm^2 for 4 min before increasing shear to 1 dyne/cm^2 for 1 min. Neutrophil interactions were visualized using phase-contrast microscopy on an inverted microscope. Experiments were visualized and recorded with a digital video camera and monitor for playback analysis at a later time. Adherent cells are defined as those that remain stationary for ≥10 s.

Cell labeling for flow cytometric analysis. 10^6 isolated neutrophils or heparanized whole blood from untreated mice (obtained via cardiac puncture) was either left untreated, incubated at 37°C for 4 h with 100 ng/ml LPS, or treated for 5 min with IRAWB14.4 to induce CD44 activation (generated as described previously [62]). In addition, peripheral blood neutrophils from mice treated with LPS for 4 h were also examined. HA binding to BM-derived neutrophils and circulating neutrophils was then assessed using FL-HA (provided by P. Johnson, University of British Columbia, Vancouver, Canada). In the case of the whole blood samples, red blood cells were lysed with OptiLyse B (Beckman Coulter). Cells were washed, resuspended in ice-cold PBS containing 1% FBS and 0.1% sodium azide, and read on a FACScan flow cytometer (Becton Dickinson) using CELLQuest Pro software (BD Biosciences).

Statistics. All data are presented as mean values ± SEM. A Student's *t* test was used to determine the significance between population means. A Bonferroni correction was used for multiple comparisons. Statistical significance was set at $P < 0.05$.

Online supplemental material. Video S1 demonstrates hepatic sinusoidal perfusion under baseline conditions and after treatment with i.v. LPS as observed via intravital microscopy. Fig. S1 depicts intravital microscopy data obtained from WT or CD44$^{-/-}$ mice left untreated, treated with LPS alone, or in combination with anti-RHAMM or anti–VAP-1 antibodies. The online supplemental material is available at http://www.jem.org/cgi/content/full/jem.20071765/DC1.

The authors would like to thank Dean Brown and Carol Gzwod for excellent technical assistance, Dr. Pina Colarusso and Ms. Brandie Millen for their assistance with the spinning disk microscopy, and Dr. Pauline Johnson for helpful discussions. We would also like to acknowledge the CIHR-funded Live Cell Imaging Facility at the Faculty of Medicine, University of Calgary.

This work was supported by the Canadian Institute of Health Research (CIHR) and the CIHR group grant. P. Kubes is an Alberta Heritage Foundation for Medical Research (AHFMR) Scientist, Canada Research Chair, and the Snyder Chair in Critical Care Medicine. B. McDonald is an AHFMR-funded trainee.

The authors have no conflicting financial interests.

Submitted: 17 August 2007
Accepted: 5 March 2008

REFERENCES

1. Bone, R.C. 1991. Sepsis, the sepsis syndrome, multi-organ failure: a plea for comparable definitions. *Ann. Intern. Med.* 114:332–333.
2. Ziegler, E.J., J.A. McCutchan, J. Fierer, M.P. Glauser, J.C. Sadoff, H. Douglas, and A.I. Braude. 1982. Treatment of gram-negative bacteremia and shock with human antiserum to a mutant Escherichia coli. *N. Engl. J. Med.* 307:1225–1230.
3. Beutler, B., Z. Jiang, P. Georgel, K. Crozat, B. Croker, S. Rutschmann, X. Du, and K. Hoebe. 2006. Genetic analysis of host resistance: Toll-like receptor signaling and immunity at large. *Annu. Rev. Immunol.* 24:353–389.
4. Welbourn, C.R., and Y. Young. 1992. Endotoxin, septic shock and acute lung injury: neutrophils, macrophages and inflammatory mediators. *Br. J. Surg.* 79:998–1003.
5. Simpson, A.J., S.M. Opal, B.J. Angus, J.M. Prins, J.E. Palardy, N.A. Parejo, W. Chaowagul, and N.J. White. 2000. Differential antibiotic-induced endotoxin release in severe melioidosis. *J. Infect. Dis.* 181:1014–1019.
6. Hopkin, B.D. 1985. A nasty shock from antibiotics? *Lancet.* 2:594.
7. Cross, A.S., and S.M. Opal. 2003. A new paradigm for the treatment of sepsis: is it time to consider combination therapy? *Ann. Intern. Med.* 138:502–505.
8. Ley, K., D.C. Bullard, M.L. Arbones, R. Bosse, D. Vestweber, T.F. Tedder, and A.L. Beaudet. 1995. Sequential contribution of L- and P-selectin to leukocyte rolling in vivo. *J. Exp. Med.* 181:669–675.
9. Lindbom, L., X. Xie, J. Raud, and P. Hedqvist. 1992. Chemoattractant-induced firm adhesion of leukocytes to vascular endothelium in vivo is critically dependent on initial leukocyte rolling. *Acta Physiol. Scand.* 146:415–421.
10. Nolte, D., P. Schmid, U. Jager, A. Botzlar, F. Roesken, R. Hecht, E. Uhl, K. Messmer, and D. Vestweber. 1994. Leukocyte rolling in venules of striated muscle and skin is mediated by P-selectin, not by L-selectin. *Am. J. Physiol.* 267:H1637–H1642.
11. Liu, L., and P. Kubes. 2003. Molecular mechanisms of leukocyte recruitment: organ-specific mechanisms of action. *Thromb. Haemost.* 89:213–220.

12. Jaeschke, H., and C.W. Smith. 1997. Cell adhesion and migration. III. Leukocyte adhesion and transmigration in the liver vasculature. *Am. J. Physiol.* 273:G1169–G1173.
13. Wong, J., B. Johnston, S.S. Lee, D.C. Bullard, C.W. Smith, A.L. Beaudet, and P. Kubes. 1997. A minimal role for selectins in the recruitment of leukocytes into the inflamed liver microvasculature. *J. Clin. Invest.* 99:2782–2790.
14. Jaeschke, H., and C.W. Smith. 1997. Mechanisms of neutrophil-induced parenchymal cell injury. *J. Leukoc. Biol.* 61:647–653.
15. Jaeschke, H., A. Farhood, M.A. Fisher, and C.W. Smith. 1996. Sequestration of neutrophils in the hepatic vasculature during endotoxemia is independent of beta 2 integrins and intercellular adhesion molecule-1. *Shock.* 6:351–356.
16. Fox-Robichaud, A., and P. Kubes. 2000. Molecular mechanisms of tumor necrosis factor alpha-stimulated leukocyte recruitment into the murine hepatic circulation. *Hepatology.* 31:1123–1127.
17. Hemler, M.E. 1990. VLA proteins in the integrin family: structures, functions, and their role on leukocytes. *Annu. Rev. Immunol.* 8:365–400.
18. Alon, R., P.D. Kassner, M.W. Carr, E.B. Finger, M.E. Hemler, and T.A. Springer. 1995. The integrin VLA-4 supports tethering and rolling in flow on VCAM-1. *J. Cell Biol.* 128:1243–1253.
19. Ibbotson, G.C., C. Doig, J. Kaur, V. Gill, L. Ostrovsky, T. Fairhead, and P. Kubes. 2001. Functional alpha4-integrin: a newly identified pathway of neutrophil recruitment in critically ill septic patients. *Nat. Med.* 7:465–470.
20. Gaboury, J.P., and P. Kubes. 1994. Reductions in physiologic shear rates lead to CD11/CD18-dependent, selectin-independent leukocyte rolling in vivo. *Blood.* 83:345–350.
21. Stokol, T., P. O'Donnell, L. Xiao, S. Knight, G. Stavrakis, M. Botto, U.H. von Andrian, and T.N. Mayadas. 2004. C1q governs deposition of circulating immune complexes and leukocyte Fcγ receptors mediate subsequent neutrophil recruitment. *J. Exp. Med.* 200:835–846.
22. Siegelman, M.H., H.C. DeGrendele, and P. Estess. 1999. Activation and interaction of CD44 and hyaluronan in immunological systems. *J. Leukoc. Biol.* 66:315–321.
23. Matsumoto, M., K. Atarashi, E. Umemoto, Y. Furukawa, A. Shigeta, M. Miyasaka, and T. Hirata. 2005. CD43 functions as a ligand for E-Selectin on activated T cells. *J. Immunol.* 175:8042–8050.
24. Bonder, C.S., M.U. Norman, M.G. Swain, L.D. Zbytnuik, J. Yamanouchi, P. Santamaria, M. Ajuebor, M. Salmi, S. Jalkanen, and P. Kubes. 2005. Rules of recruitment for Th1 and Th2 lymphocytes in inflamed liver: a role for alpha-4 integrin and vascular adhesion protein-1. *Immunity.* 23:153–163.
25. Nandi, A., P. Estess, and M. Siegelman. 2004. Bimolecular complex between rolling and firm adhesion receptors required for cell arrest; CD44 association with VLA-4 in T cell extravasation. *Immunity.* 20:455–465.
26. Bonder, C.S., S.R. Clark, M.U. Norman, P. Johnson, and P. Kubes. 2006. Use of CD44 by CD4+ Th1 and Th2 lymphocytes to roll and adhere. *Blood.* 107:4798–4806.
27. Zhuo, L., A. Kanamori, R. Kannagi, N. Itano, J. Wu, M. Hamaguchi, N. Ishiguro, and K. Kimata. 2006. SHAP potentiates the CD44-mediated leukocyte adhesion to the hyaluronan substratum. *J. Biol. Chem.* 281:20303–20314.
28. Parker, J.C., M.A. Perry, and A.E. Taylor. 1984. Permeability of the microvascular barrier. *In* Edema. N.C. Staub and A.E. Taylor, editors. Raven, New York. 143–187.
29. Zaman, A., Z. Cui, J.P. Foley, H. Zhao, P.C. Grimm, H.M. Delisser, and R.C. Savani. 2005. Expression and role of the hyaluronan receptor RHAMM in inflammation after bleomycin injury. *Am. J. Respir. Cell Mol. Biol.* 33:447–454.
30. Nedvetzki, S., E. Gonen, N. Assayag, R. Reich, R.O. Williams, R.L. Thurmond, J.F. Huang, B.A. Neudecker, F.S. Wang, E.A. Turley, and D. Naor. 2004. RHAMM, a receptor for hyaluronan-mediated motility, compensates for CD44 in inflamed CD44-knockout mice: a different interpretation of redundancy. *Proc. Natl. Acad. Sci. USA.* 101:18081–18086.
31. Lesley, J., Q. He, K. Miyake, A. Hamann, R. Hyman, and P.W. Kincade. 1992. Requirements for hyaluronic acid binding by CD44: a role for the cytoplasmic domain and activation by antibody. *J. Exp. Med.* 175:257–266.
32. de la Motte, C.A., V.C. Hascall, J. Drazba, S.K. Bandyopadhyay, and S.A. Strong. 2003. Mononuclear leukocytes bind to specific hyaluronan structures on colon mucosal smooth muscle cells treated with polyinosinic acid:polycytidylic acid: inter-alpha-trypsin inhibitor is crucial to structure and function. *Am. J. Pathol.* 163:121–133.
33. Li, Y., D.A. Muruve, R.G. Collins, S.S. Lee, and P. Kubes. 2002. The role of selectins and integrins in adenovirus vector-induced neutrophil recruitment to the liver. *Eur. J. Immunol.* 32:3443–3452.
34. Klintman, D., R. Schramm, M.D. Menger, and H. Thorlacius. 2002. Leukocyte recruitment in hepatic injury: selectin-mediated leukocyte rolling is a prerequisite for CD18-dependent firm adhesion. *J. Hepatol.* 36:53–59.
35. Shappell, S.B., C. Toman, D.C. Anderson, A.A. Taylor, M.L. Entman, and C.W. Smith. 1990. Mac-1 (CD11b/CD18) mediates adherence-dependent hydrogen peroxide production by human and canine neutrophils. *J. Immunol.* 144:2702–2711.
36. Poon, B.Y., C.A. Ward, C.B. Cooper, W.R. Giles, A.R. Burns, and P. Kubes. 2001. alpha(4)-integrin mediates neutrophil-induced free radical injury to cardiac myocytes. *J. Cell Biol.* 152:857–866.
37. Labow, M.A., C.R. Norton, J.M. Rumberger, K.M. Lombard-Gillooly, D.J. Shuster, J. Hubbard, R. Bertko, P.A. Knaack, R.W. Terry, M.L. Harbison, et al. 1994. Characterization of E-selectin-deficient mice: demonstration of overlapping function of the endothelial selectins. *Immunity.* 1:709–720.
38. Staite, N.D., J.M. Justen, I.M. Sly, A.I. Deaudet, and D.C. Bullard. 1996. Inhibition of delayed-type contact hypersensitivity in mice deficient in both E-selectin and P-selectin. *Blood.* 88:2973–2979.
39. Hwang, J., J. Yamanouchi, P. Santamaria, and P. Kubes. 2004. A critical temporal window for selectin-dependent $CD4^+$ lymphocyte homing and initiation of late phase inflammation in contact sensitivity. *J. Exp. Med.* 199:1223–1234.
40. Erzurum, S.C., G.P. Downey, D.E. Doherty, B. Schwab III, E.L. Elson, and G.S. Worthen. 1992. Mechanisms of lipopolysaccharide-induced neutrophil retention. Relative contributions of adhesive and cellular mechanical properties. *J. Immunol.* 149:154–162.
41. Khan, A.I., S.M. Kerfoot, B. Heit, L. Liu, G. Andonegui, B. Ruffell, P. Johnson, and P. Kubes. 2004. Role of CD44 and hyaluronan in neutrophil recruitment. *J. Immunol.* 173:7594–7601.
42. DeGrendele, H.C., P. Estess, and M.H. Siegelman. 1997. Requirement for CD44 in activated T cell extravasation into an inflammatory site. *Science.* 278:672–675.
43. Satoh, T., T. Ichida, Y. Matsuda, M. Sugiyama, K. Yonekura, T. Ishikawa, and H. Asakura. 2000. Interaction between hyaluronan and CD44 in the development of dimethylnitrosamine-induced liver cirrhosis. *J. Gastroenterol. Hepatol.* 15:402–411.
44. Ichida, T., S. Sugitani, T. Satoh, Y. Matsuda, M. Sugiyama, K. Yonekura, T. Ishikawa, and H. Asakura. 1996. Localization of hyaluronan in human liver sinusoids: a histochemical study using hyaluronan-binding protein. *Liver.* 16:365–371.
45. Mohamadzadeh, M., H. DeGrendele, H. Arizpe, P. Estess, and M. Siegelman. 1998. Proinflammatory stimuli regulate endothelial hyaluronan expression and CD44/HA-dependent primary adhesion. *J. Clin. Invest.* 101:97–108.
46. Nandi, A., P. Estess, and M.H. Siegelman. 2000. Hyaluronan anchoring and regulation on the surface of vascular endothelial cells is mediated through the functionally active form of CD44. *J. Biol. Chem.* 275:14939–14948.
47. Zhou, B., J.A. Weigel, L. Fauss, and P.H. Weigel. 2000. Identification of the hyaluronan receptor for endocytosis (HARE). *J. Biol. Chem.* 275:37733–37741.
48. Weigel, J.A., R.C. Raymond, C. McGary, A. Singh, and P.H. Weigel. 2003. A blocking antibody to the hyaluronan receptor for endocytosis (HARE) inhibits hyaluronan clearance by perfused liver. *J. Biol. Chem.* 278:9808–9812.
49. Levesque, M.C., and B.F. Haynes. 1997. Cytokine induction of the ability of human monocyte CD44 to bind hyaluronan is mediated primarily by TNF-alpha and is inhibited by IL-4 and IL-13. *J. Immunol.* 159:6184–6194.
50. Pure, E., and C.A. Cuff. 2001. A crucial role for CD44 in inflammation. *Trends Mol. Med.* 7:213–221.

51. Lesley, J., V.C. Hascall, M. Tammi, and R. Hyman. 2000. Hyaluronan binding by cell surface CD44. *J. Biol. Chem.* 275:26967–26975.
52. Cattaruzza, S., M. Schiappacassi, K. Kimata, A. Colombatti, and R. Perris. 2004. The globular domains of PG-M/versican modulate the proliferation-apoptosis equilibrium and invasive capabilities of tumor cells. *FASEB J.* 18:779–781.
53. Phillipson, M., B. Heit, P. Colarusso, L. Liu, C.M. Ballantyne, and P. Kubes. 2006. Intraluminal crawling of neutrophils to emigration sites: a molecularly distinct process from adhesion in the recruitment cascade. *J. Exp. Med.* 203:2569–2575.
54. Clark, S.R., A.C. Ma, S.A. Tavener, B. McDonald, Z. Goodarzi, M.M. Kelly, K.D. Patel, S. Chakrabarti, E. McAvoy, G.D. Sinclair, et al. 2007. Platelet TLR4 activates neutrophil extracellular traps to ensnare bacteria in septic blood. *Nat. Med.* 13:463–469.
55. Schmits, R., J. Filmus, N. Gerwin, G. Senaldi, F. Kiefer, T. Kundig, A. Wakeham, A. Shahinian, C. Catzavelos, J. Rak, et al. 1997. CD44 regulates hematopoietic progenitor distribution, granuloma formation, and tumorigenicity. *Blood.* 90:2217–2233.
56. Hickey, M.J., D.N. Granger, and P. Kubes. 1999. Molecular mechanisms underlying IL-4-induced leukocyte recruitment in vivo: a critical role for the alpha 4 integrin. *J. Immunol.* 163:3441–3448.
57. Eppihimer, M.J., B. Wolitzky, D.C. Anderson, M.A. Labow, and D.N. Granger. 1996. Heterogeneity of expression of E- and P-selectins in vivo. *Circ. Res.* 79:560–569.
58. Carvalho-Tavares, J., M.J. Hickey, J. Hutchison, J. Michaud, I.T. Sutcliffe, and P. Kubes. 2000. A role for platelets and endothelial selectins in tumor necrosis factor-alpha-induced leukocyte recruitment in the brain microvasculature. *Circ. Res.* 87:1141–1148.
59. Bonder, C.S., M.N. Ajuebor, L.D. Zbytnuik, P. Kubes, and M.G. Swain. 2004. Essential role for neutrophil recruitment to the liver in concanavalin A-induced hepatitis. *J. Immunol.* 172:45–53.
60. Kerfoot, S.M., M.U. Norman, B.M. Lapointe, C.S. Bonder, L. Zbytnuik, and P. Kubes. 2006. Reevaluation of P-selectin and alpha 4 integrin as targets for the treatment of experimental autoimmune encephalomyelitis. *J. Immunol.* 176:6225–6234.
61. Johnsson, C., R. Hallgren, A. Elvin, B. Gerdin, and G. Tufveson. 1999. Hyaluronidase ameliorates rejection-induced edema. *Transpl. Int.* 12:235–243.
62. Li, R., J.R. Walker, and P. Johnson. 1998. Chimeric CD4/CD44 molecules associate with CD44 via the transmembrane region and reduce hyaluronan binding in T cell lines. *Eur. J. Immunol.* 28:1745–1754.